Identification of BSPRY as a Novel Auxiliary Protein Inhibiting TRPV5 Activity

Stan F.J. van de Graaf, Annemiete W.C.M. van der Kemp, Dennis van den Berg, Mijke van Oorschot, Joost G.J. Hoenderop, and René J.M. Bindels

Department of Physiology, Nijmegen Centre for Molecular Life Sciences, Radboud University Nijmegen Medical Centre, Nijmegen, The Netherlands

Transient receptor potential vallinoid 5 (TRPV5) and TRPV6 are the most Ca^{2+}-selective members of the TRP superfamily and are essential for active Ca^{2+} (re)absorption in epithelia. However, little is known about intracellular proteins that regulate the activity of these channels. This study identified BSPRY (B-box and SPRY-domain containing protein) as a novel factor involved in the control of TRPV5. The interaction between BSPRY and TRPV5 by GST pull-down and co-immunoprecipitation assays was demonstrated. BSPRY showed co-localization with TRPV5 in mouse kidney. Expression of BSPRY resulted in a significant reduction of the Ca^{2+} influx in Madin-Darby Canine Kidney cells that stably express TRPV5 without affecting channel cell-surface abundance. Finally, BSPRY expression in kidney was increased in 25-hydroxyvitamin D_3-1α-hydroxylase knockout mice, suggesting an inverse regulation by vitamin D_3. Together, these results demonstrate the physiologic role of the novel protein BSPRY in the regulation of epithelial Ca^{2+} transport *via* negative modulation of TRPV5 activity.

J Am Soc Nephrol 17: 26–30, 2006. doi: 10.1681/ASN.2005101025

The epithelial Ca^{2+} channels transient receptor potential vallinoid 5 (TRPV5) and TRPV6 form two highly Ca^{2+}-permeable members of the TRP superfamily of cation channels. Recent studies using TRPV5 knockout mice have demonstrated the pivotal gatekeeper role of TRPV5 in active Ca^{2+} reabsorption (1). These mice show a robust renal Ca^{2+} loss and display considerable bone abnormalities. In addition, TRPV5 knockout mice exhibit a significant Ca^{2+} hyperabsorption, associated with an increased duodenal TRPV6 expression level, resulting from elevated 1,25-dihydroxyvitamin D_3 levels (1,2). The preliminary characterization of TRPV6 knockout mice showed decreased intestinal Ca^{2+} absorption and bone mineral density, further substantiating the role of this channel in intestinal Ca^{2+} absorption (3). Together, TRPV5 and TRPV6 form the gatekeepers of transcellular Ca^{2+} transport, and understanding their regulation is pivotal for our insight into the (patho)physiology of Ca^{2+} homeostasis (4). However, the molecular mechanisms underlying channel trafficking and regulation of its activity at the plasma membrane are incompletely understood.

The aim of this study, therefore, was to identify proteins that modulate the activity of TRPV5 or TRPV6 to regulate transcellular Ca^{2+} transport. Here, we describe the identification of BSPRY (B-box and SPRY-domain containing protein), a novel protein with previously unknown function, as a channel-associated regulatory protein of the epithelial Ca^{2+} channel TRPV5.

Published online ahead of print. Publication date available at www.jasn.org.

Address correspondence to: Dr. René J.M. Bindels, 286 Cell Physiology, Radboud University Nijmegen Medical Centre, PO Box 9101, NL-6500 HB Nijmegen, The Netherlands. Phone: +31-24-361-4211; Fax: +31-24-361-6413; E-mail: r.bindels@ncmls.ru.nl

Materials and Methods

DNA Constructs and cRNA Synthesis

Full-length BSPRY was obtained from mouse expressed sequence tag (EST) I.M.A.G.E. 5116439, cloned into the pTLN oocyte expression vector (5) in frame with an amino-terminal VSV tag and subcloned into pGEX6p2 (Amersham Biosciences, Uppsala, Sweden) and pCB7 (6). Full-length and carboxyl-termini of TRPV5 and TRPV6 were obtained as described previously (7).

Yeast Two-Hybrid System

Y153 yeast strain transformation and subsequently screening of a mouse kidney cDNA library (Clontech, Palo Alto, CA) was performed as described previously (7).

Protein–Protein Interaction Assays

Glutathione S-transferase (GST) fusion proteins were expressed in *Escherichia coli* BL21 and purified according to the manufacturer's protocol (Amersham Biosciences). BSPRY cRNA was synthesized *in vitro* using SP6 RNA polymerase as described previously (7) and injected into *Xenopus laevis* oocytes. After 2 d, oocytes were lysed in PBS that contained 0.4% (vol/vol) Triton X-100. [^{35}S]Methionine-labeled full-length TRPV5/TRPV6 protein was prepared using a reticulocyte lysate system. *Xenopus* oocyte lysates or *in vitro*–translated proteins were incubated with GST or GST-fusion proteins that were immobilized on glutathione-Sepharose 4B beads (Amersham Biosciences) in PBS that contained 0.4% (vol/vol) Triton X-100 for 2 h at room temperature, and bound proteins were visualized by autoradiography or immunoblotting. MDCK cells that were stably transfected with green fluorescent protein (GFP)-fused TRPV5 and VSV-BSPRY were lysed in sucrose buffer that fused contained 20 mM Tris (pH 7.4), 5 mM EDTA, 135 mM NaCl, 0.5% (vol/vol) NP-40, 0.2% (vol/vol) Triton X-100, and 10% (wt/vol) sucrose, incubated on ice for 60 min, and centrifuged for 30 min at 16,000 $\times$ *g*. Supernatants were incubated with guinea pig anti-TRPV5 or monoclonal anti-VSV antibodies (Sigma, St. Louis, MO)

ISSN: 1046-6673/1701-0026

immobilized on protein A-agarose beads (Kem-En-Tec A/S, Copenhagen, Denmark) for 16 h at 4°C. Immunoprecipitated proteins were analyzed by immunoblot analysis.

Reverse Transcription–PCR Analysis

Total RNA was isolated using TRIzol (Life Technologies/BRL, Life Technologies, Breda, The Netherlands). Total RNA (2 μg) was subjected to reverse transcription (RT) using Moloney murine leukemia virus reverse transcriptase, and a PCR for BSPRY was performed using the primers 5′-GATTCGGAGAAATTAAGC-3′ and 5′-GGCTGCAGTTACAGAGTGC-3′. BSPRY mRNA expression was quantified by real-time PCR using SYBRGreen dye and shown as relative expression to mouse hypoxanthine-guanine phosphoribosyl transferase (detected with the forward primer 5′-TTATCAGACTGAAGAGCTACTGTAATGATC-3′, reverse primer 5′-TTACCAGTGTCAATTATATCTTCAACAATC-3′), which was used as an endogenous control to normalize variations in RNA extractions, the degree of RNA degradation, and variabilities in RT efficiencies. The primers that were used to amplify β-actin were 5′-ACCATTTCCCTCTCAGCTGTG-3′ and 5′-GTATGCCTCTGGTCGTACCAC-3′.

Preparation of Antibodies and Immunohistochemistry

Rabbit anti-BSPRY antibodies were raised against the peptide H_2N-LFPVFAVADQLISIV-COOH of mouse BSPRY and used for immunohistochemistry as described. For semiquantitative determination of protein levels, images were analyzed with Image J (http://rsb.info.nih.gov/ij/), resulting in quantification of the protein levels as the mean of integrated optical density as described (2). All negative controls, including preimmune serum and serum depleted of anti-BSPRY antibodies by incubation for 16 h with GST-BSPRY immobilized on glutathione-Sepharose 4B beads, were devoid of staining.

$^{45}Ca^{2+}$ Uptake Assay

Ca^{2+} uptake was determined using MDCK cells by incubation in uptake medium that contained 1.0 mM $CaCl_2$ for 5 min at room temperature as described previously.

Cell-Surface Biotinylation

Proteins that were present at the cell surface of confluent stably transfected MDCK cells were biotinylated at 4°C using NHS-LC-LC-biotin (0.5 mg/ml; Pierce, Etten-Leur, The Netherlands), precipitated using neutravidin-coupled beads (Pierce), and analyzed by immunoblot analyses.

Statistical Analyses

In all experiments, the data are expressed as mean ± SEM. Overall statistical significance was determined by ANOVA. $P < 0.05$ was considered significant.

Results and Discussion

Our study provides the first evidence of the physiologic role of BSPRY as a negative modulator of the epithelial Ca^{2+} channel TRPV5. This conclusion is based on four independent observations. First, the specific interaction between this channel and BSPRY was demonstrated by yeast two-hybrid, GST pull-down and co-immunoprecipitation assays. Second, BSPRY showed complete co-localization with TRPV5 in Ca^{2+}-transporting tubular segments of the kidney. Third, stable expression of BSPRY significantly inhibited Ca^{2+} influx in confluent layers of MDCK cells expressing TRPV5. Fourth, BSPRY expression was inversely regulated by the calciotropic hormone vitamin D_3.

Identification of BSPRY as a Novel TRPV5- and TRPV6-Associated Protein

To discover novel TRPV5- and TRPV6-associated proteins, we performed a yeast two-hybrid screen on a mouse kidney cDNA library. Using the mouse TRPV6 carboxyl-terminus as bait, five clones that were identified as BSPRY were isolated. BSPRY contains a B-box and SPRY domain, whose tentative functions are protein–protein interaction modules (8,9). The association of full-length BSPRY with GST-TRPV5 or TRPV6 carboxyl-termini, immobilized on Sepharose 4B beads, confirmed the yeast two-hybrid results and showed that TRPV5 (Figure 1A) also interacts with BSPRY (Figure 1A). Furthermore, the reverse approach, whereby full-length, GST-fused BSPRY was immobilized on Sepharose beads and incubated with *in vitro*–translated full-length TRPV5 or TRPV6, resulted in significant binding of both Ca^{2+} channels to BSPRY (Figure 1B). The binding of BSPRY was equal in the presence of 1 mM Ca^{2+} or in Ca^{2+}-free (2 mM EDTA) conditions, demonstrating a Ca^{2+}-independent association (data not shown). No interaction was observed with GST alone, indicating the specificity of the binding.

To substantiate further the BSPRY interaction, we generated MDCK cell lines that were stably transfected with GFP-fused TRPV5 and subsequently with VSV-BSPRY or the empty pCB7 vector. These cell lines allowed the investigation of TRPV5 in a polarized epithelium, whereas endogenous expression levels of these channels in native tissues, including kidney, were below the detection limit of immunoblot analysis. Furthermore, these polarized cells exhibit apical uptake of Ca^{2+} and provide a valuable model to study TRPV5-mediated Ca^{2+} influx (10). Using these stably transfected cells, TRPV5 could be co-immunoprecipitated with anti-VSV antibodies upon expression of VSV-BSPRY, as indicated by the specific bands at approximately 95 kD for the core-glycosylated GFP-TRPV5 and approximately 115 kD for complex-glycosylated GFP-TRPV5 (Figure 1C). TRPV5 was not detected in the immunoprecipitated sample in the absence of VSV-BSPRY, confirming the specificity of the procedure. Similarly, BSPRY was co-immunoprecipitated with TRPV5 in the reverse reaction using anti-TRPV5 antibodies that were immobilized on Sepharose beads, as represented by an immunopositive band of approximately 65 kD (Figure 1D). Here, β-actin was used as a control to demonstrate equal input of the samples. β-Actin was absent in the immunoprecipitated sample, indicating the specificity of the interaction.

Co-Localization of BSPRY and TRPV5

The expression of BSPRY in mouse tissues was analyzed by RT-PCR. BSPRY was detected in several tissues, including kidney, small intestine, prostate, lung, and uterus. BSPRY was less abundantly expressed in heart, whereas skeletal muscle and liver were negative (Figure 2A, top). All samples expressed β-actin, which was used as a positive control to confirm cDNA integrity (Figure 2A, bottom). Using anti-BSPRY antibodies, raised in rabbits using a conserved 15–amino acid peptide of the carboxyl-terminus of mouse BSPRY, we demonstrated that

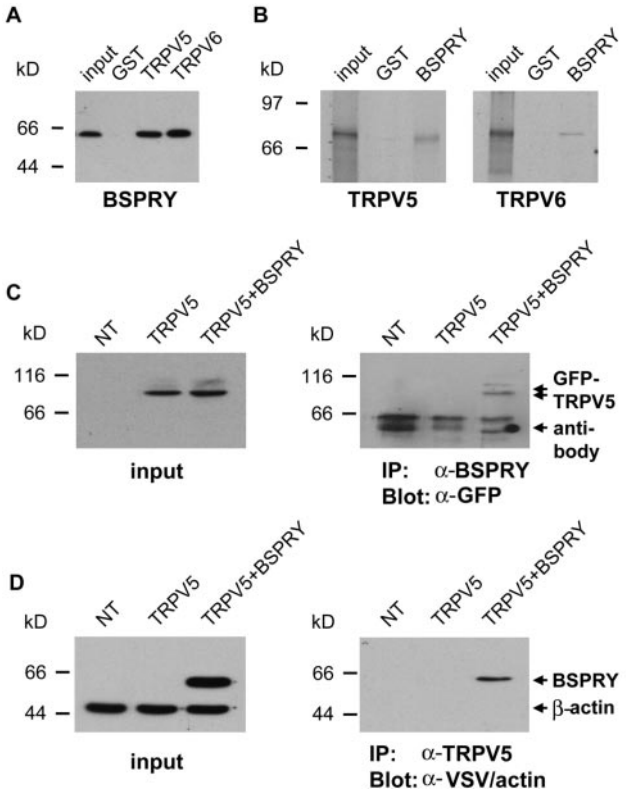

Figure 1. Interaction of transient receptor potential vallinoid 5 (TRPV5) or TRPV6 with BSPRY (B-box and SPRY-domain containing protein) as shown by glutathione S-transferase (GST) pull-down and co-immunoprecipitation analyses. (A) Lysates of *Xenopus laevis* oocytes that were injected with 10 ng of VSV-tagged BSPRY cRNA were incubated with GST or GST fused to the carboxyl-terminus of TRPV5 or TRPV6 immobilized on glutathione-Sepharose 4B beads. BSPRY interacted specifically with TRPV5 and TRPV6 but not with GST alone. (B) [^{35}S]Methionine-labeled full-length TRPV5 or TRPV6 was incubated with GST or GST-BSPRY immobilized on glutathione-Sepharose 4B beads. Both TRPV5 and TRPV6 interacted with BSPRY, whereas no binding to GST alone was observed. (C) MDCK cells that stably expressed green fluorescent protein (GFP)-fused TRPV5 were transfected with pCB7-VSV-BSPRY of the empty pCB7 vector, and five clones with equal growth rate and TRPV5 expression of both conditions were pooled to eliminate clonal variation. MDCK lysates were incubated with anti-VSV antibodies. Co-immunoprecipitated TRPV5 was demonstrated using anti-GFP antibodies. TRPV5 could not be precipitated in the absence of BSPRY (right), although TRPV5 expression was similar in both conditions (left), demonstrating the specificity of the interaction. (D) Expression of VSV-BSPRY was determined by immunoblot analysis using monoclonal anti-VSV. Expression of β-actin was used to show equal loading. Lysates were subjected to immunoprecipitation using anti-TRPV5 antibodies. Co-immunoprecipitated BSPRY was demonstrated by immunoblot analysis using anti-VSV antibodies. β-Actin was not co-immunoprecipitated, showing the specificity of the interaction. None-transfected MDCK cells (NT) were used to demonstrate the specificity of the antibodies.

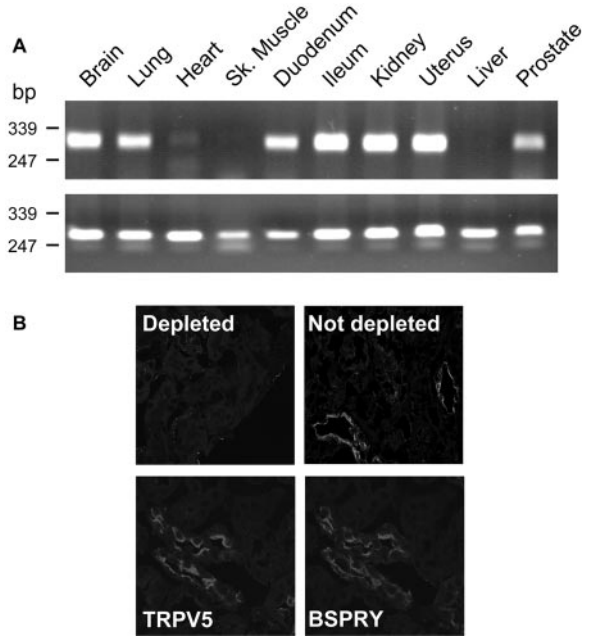

Figure 2. Localization and tissue distribution of BSPRY. (A) RNA was extracted from several mouse tissues, and BSPRY expression was determined by reverse transcription–PCR. The BSPRY-specific band was amplified in brain, lung, duodenum, ileum, kidney, prostate, and uterus (top). A faint signal was detected in heart, whereas skeletal muscle and liver were negative (top). β-Actin was used as a control to ensure cDNA integrity and was positive in all tested tissues (bottom). (B) Immunohistochemical analysis of BSPRY and TRPV5 in mouse kidney sections. To verify the specificity of the BSPRY antibody, we incubated polyclonal rabbit BSPRY antiserum for 16 h with GST-BSPRY, immobilized on glutathione-Sepharose 4B beads. Depletion of the BSPRY antibodies abolished all immunopositive signal, whereas incubation with immobilized GST alone (not depleted) did not affect the reactivity of the antiserum. Furthermore, kidney sections were co-stained with antibodies against BSPRY and TRPV5. BSPRY and TRPV5 have a remarkable similarity in localization and show significant overlap in the apical region of the cell. No signal was detected with preimmune serum or with fluorophore-conjugated antibodies only.

the localization of BSPRY in kidney is strikingly similar to the localization of TRPV5 (Figure 2B, bottom). BSPRY was present in the apical domain of all TRPV5-immunopositive tubules, previously identified as the second part of the distal convoluted tubule and connecting tubule (11,12). Proximal tubules and glomeruli were negative, and preimmune serum did not show any staining. Furthermore, immunopositive BSPRY staining was absent upon incubation of the serum with immobilized GST-BSPRY, whereas incubation with GST alone had no effect (Figure 2B, top). Similar co-localization with TRPV5 in distal convoluted tubule and connecting tubule was observed previously for calbindin-D_{28K} and the Na^+/Ca^{2+} exchanger (12,13). These proteins play an essential role in renal transcellular Ca^{2+} transport as they respectively facilitate the diffusion of Ca^{2+} from the apical to the basolateral side and the extrusion into the blood. Similarly, the robust co-localization between BSPRY and TRPV5 strongly supports a physiologic and specific function of BSPRY in the regulation of epithelial Ca^{2+} transport by direct association with TRPV5 in the kidney.

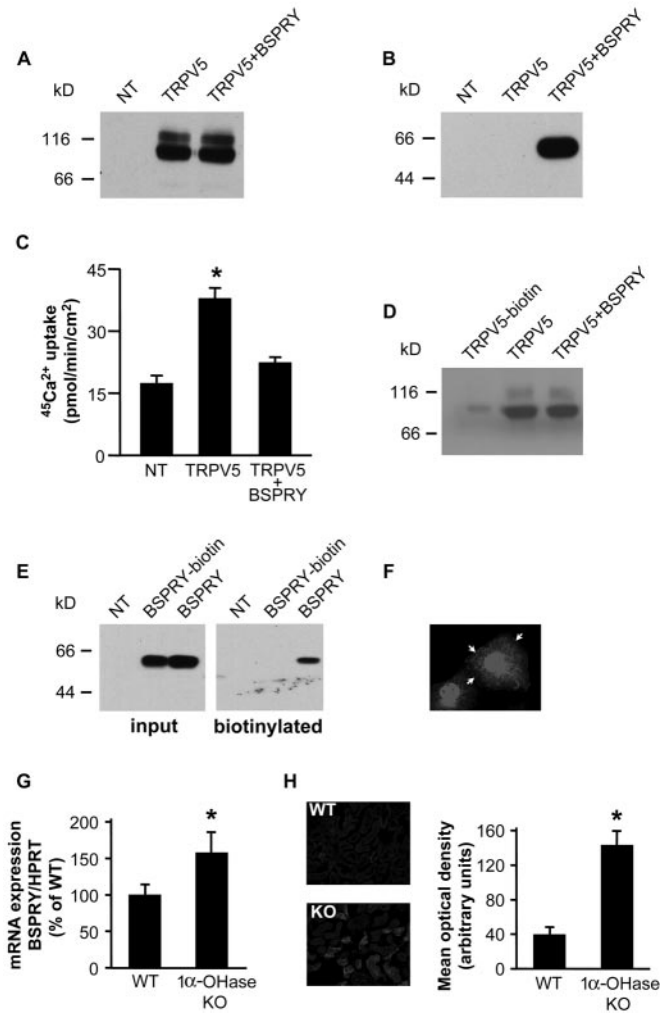

Figure 3. BSPRY operates as a negative modulator of TRPV5 activity. (A) The expression level of GFP-tagged TRPV5 in stably transfected MDCK cells was determined by immunoblot using anti-GFP antibodies and shows equal expression levels in the presence or absence of BSPRY. (B) BSPRY expression was verified using monoclonal anti-VSV antibodies. (C) TRPV5 activity was determined by radioactive Ca^{2+} uptake in MDCK cells that were grown to confluence, demonstrating a significant inhibition of TRPV5-mediated Ca^{2+} influx upon BSPRY co-expression. (D) Intact GFP-TRPV5–expressing MDCK cells, stably transfected with pCB7-VSV-BSPRY or the empty pCB7 vector, were incubated with NHS-LC-LC-biotin to label cell-surface proteins. Biotinylated proteins were isolated using neutravidin-agarose beads, separated by SDS-PAGE, and TRPV5 was subsequently quantified by immunoblot analysis. TRPV5 plasma membrane abundance was equal in the presence or absence of BSPRY. TRPV5 and BSPRY were not detected in precipitates from cells that were not exposed to biotin, showing the specificity of the precipitation for biotinylated proteins. Similarly, BSPRY was detected in the plasma membrane by biotinylation (E) and immunocytochemistry (F, arrowheads) using anti-VSV antibodies on stably BSPRY-transfected MDCK cells. β-Actin was found in the lysate from the biotinylated MDCK monolayers but not in the fraction recovered from the neutravidin beads, demonstrating that intracellular proteins are not isolated using this procedure (data not shown). *$P < 0.05$ *versus* all. (G) The role of vitamin D_3 on BSPRY expression was determined by quantitative real-time PCR in kidneys of wild-type (WT; $n = 11$) or 25-hydroxyvitamin D_3-1α-hydroxylase (1α-OHase) knockout (KO; $n = 6$) mice. (H) Effect of vitamin D_3 on BSPRY protein abundance in mouse kidney. Representative images showing kidney sections stained for BSPRY in WT or 1α-OHase KO mice. Protein abundance was determined by computerized analysis of immunohistochemical images and is presented as mean optical density (arbitrary units) for $n = 24$ to 30 pictures from five mice for each condition. *$P < 0.05$ *versus* WT.

BSPRY-Mediated TRPV5 Inhibition of Ca^{2+} Influx

The effect of BSPRY co-expression on TRPV5-mediated Ca^{2+} influx was measured using confluent monolayers of MDCK cells. TRPV5 expression in these cells resulted in an approximately 2.5-fold increased Ca^{2+} influx compared with nontransfected cells. Upon co-expression with BSPRY, Ca^{2+} influx was inhibited by 41 ± 13% (Figure 3C), approaching levels of nontransfected cells. Total cellular TRPV5 expression levels were identical in the presence or absence of BSPRY, as was demonstrated by immunoblot analysis using anti-GFP antibodies (Figure 3, A and B). Furthermore, the correct size of the bands at approximately 95 to 115 kD in Figure 3A confirmed the integrity of the GFP-TRPV5 fusion protein. Finally, flow cytometry analysis of the GFP signal showed that >98% of the MDCK cells forming the confluent monolayer contributed to the TRPV5-dependent Ca^{2+} influx, both in the presence and in the absence of BSPRY (data not shown). These data provide the first evidence of a functional role of BSPRY. So far, only two studies have provided information about BSPRY. First, BSPRY was identified recently in a yeast two-hybrid screen using zyxin as bait. In epithelial cells, zyxin is involved in the formation of cell–cell contacts, which require actin cytoskeleton rearrangements (14). Schenker *et al.* (15) provided no data about the localization and function of BSPRY. However, the association with zyxin might hint at a role of the cytoskeleton in the BSPRY-mediated regulation of TRPV5. Second, it was shown that BSPRY interacts with 14-3-3 proteins. Although the exact role of 14-3-3 proteins remains to be elucidated fully, their role in the recognition of phosphorylated proteins is well established (16). It has been demonstrated that 14-3-3 proteins bind to specific motifs that contain a phosphorylated serine residue and have been implicated in the binding to and activation of signaling proteins (16,17). Furthermore, a role of 14-3-3 proteins in K^+ channel trafficking was postulated (18). However, cell-surface biotinylation did not provide evidence for TRPV5 trafficking as an explanation for the observed inhibitory function of BSPRY (Figure 3D). Furthermore, we demonstrated that a significant fraction of BSPRY is membrane associated and present at the plasma membrane (Figure 3, E and F, Supplemental Figure). Therefore, it is tempting to speculate that BSPRY is involved in inhibitory signaling cascades that control the activity of the epithelial Ca^{2+} channels at the cell surface.

Vitamin D–Dependent Regulation of BSPRY Expression in Kidney

It was demonstrated previously that TRPV5 expression is strongly regulated by 1,25-dihydroxyvitamin D_3, the biologic active form of vitamin D (4,19). Therefore, we assessed the expression of BSPRY in wild-type and 25-hydroxyvitamin D_3-1α-hydroxylase (1α-OHase) knockout mice. These knockout mice are unable to syn-

thesize 1,25-dihydroxyvitamin D_3 and are a valuable animal model to study vitamin D deficiency rickets type I (20). Quantitative real-time PCR showed significantly enhanced BSPRY mRNA expression in the 1α-OHase knockout mice compared with wild-type mice, suggesting that vitamin D negatively regulates the BSPRY expression (Figure 3G). Because the antibodies that we generated did not recognize BSPRY on immunoblot, the protein expression of BSPRY in these animals was semiquantified by immunohistochemistry. Depicted in Figure 3H are representative images of BSPRY expression in wild-type and 1α-OHase knockout mice. Computerized analysis of the immunohistochemical staining showed significantly enhanced BSPRY protein expression in the 1α-OHase knockout mice compared with wild-type mice, confirming the inverse regulation of BSPRY expression by circulating vitamin D on the protein level (Figure 3H). Together with the Ca^{2+} uptake results, this suggests that BSPRY operates as a negative modulator for TRPV5 and that this mechanism will be downregulated when vitamin D levels increase to stimulate active Ca^{2+} transport. These findings demonstrate a novel target for vitamin D_3 in the regulation of active Ca^{2+} transport and provide new insight into the factors involved in the Ca^{2+}-related (patho-)physiology.

Conclusion

We have identified BSPRY as a novel auxiliary protein of the epithelial Ca^{2+} channels. The association, co-localization, and functional analyses described in this study demonstrate the first physiologic role of the novel protein BSPRY in the direct regulation of TRPV5.

Acknowledgments

This work was supported by the Dutch Organization of Scientific Research (Zon-MW 016.006.001) and the Human Frontier Science Program RGP 32/2004.

References

1. Hoenderop JG, van Leeuwen JP, van der Eerden BC, Kersten FF, van der Kemp AW, Merillat AM, Waarsing JH, Rossier BC, Vallon V, Hummler E, Bindels RJ: Renal Ca2+ wasting, hyperabsorption, and reduced bone thickness in mice lacking TRPV5. *J Clin Invest* 112: 1906–1914, 2003
2. Renkema KY, Nijenhuis T, van der Eerden BC, van der Kemp AW, Weinans H, van Leeuwen JP, Bindels RJ, Hoenderop JG: Hypervitaminosis D mediates compensatory Ca2+ hyperabsorption in TRPV5 knockout mice. *J Am Soc Nephrol* 16, 3188–3195, 2005
3. Bianco S, Peng JB, Takanaga H, Kos CH, Crescenzi A, Brown EM, Hediger MA: Mice lacking the epithelial calcium channel CaT1 (TRPV6) show a deficiency in intestinal calcium absorption despite high plasma levels of 1,25-dihydroxyvitamin D. *FASEB J* 18: A706, 2004
4. Hoenderop JG, Nilius B, Bindels RJ: Calcium absorption across epithelia. *Physiol Rev* 85: 373–422, 2005
5. Steinmeyer K, Schwappach B, Bens M, Vandewalle A, Jentsch TJ: Cloning and functional expression of rat CLC-5, a chloride channel related to kidney disease. *J Biol Chem* 270: 31172–31177, 1995
6. Brewer CB, Roth MG: A single amino acid change in the cytoplasmic domain alters the polarized delivery of influenza virus hemagglutinin. *J Cell Biol* 114: 413–421, 1991
7. Van de Graaf SF, Hoenderop JG, Gkika D, Lamers D, Prenen J, Rescher U, Gerke V, Staub O, Nilius B, Bindels RJ: Functional expression of the epithelial Ca2+ channels (TRPV5 and TRPV6) requires association of the S100A10-annexin 2 complex. *EMBO J* 22: 1478–1487, 2003
8. Borden KL: RING fingers and B-boxes: Zinc-binding protein-protein interaction domains. *Biochem Cell Biol* 76: 351–358, 1998
9. Ponting C, Schultz J, Bork P: SPRY domains in ryanodine receptors Ca^{2+}-release channels. *Trends Biochem Sci* 22: 193–194, 1997
10. Den Dekker E, Schoeber J, Topala C, van de Graaf SF, Hoenderop JG, Bindels RJ: Characterization of a Madin-Darby Canine Kidney cell line stably expressing TRPV5. *Pflugers Arch* 450: 236–244, 2005
11. Loffing J, Loffing-Cueni D, Valderrabano V, Klausli L, Hebert SC, Rossier BC, Hoenderop JG, Bindels RJ, Kaissling B: Distribution of transcellular calcium and sodium transport pathways along mouse distal nephron. *Am J Physiol Renal Physiol* 281: F1021–F1027, 2001
12. Hoenderop JG, Hartog A, Stuiver M, Doucet A, Willems PH, Bindels RJ: Localization of the epithelial Ca2+ channel in rabbit kidney and intestine. *J Am Soc Nephrol* 11: 1171–1178, 2000
13. Hoenderop JG, Dardenne O, Van Abel M, Van Der Kemp AW, Van Os CH, St-Arnaud R, Bindels RJ: Modulation of renal Ca2+ transport protein genes by dietary Ca2+ and 1,25-dihydroxyvitamin D_3 in 25-hydroxyvitamin D3–1alpha-hydroxylase knockout mice. *FASEB J* 16: 1398–1406, 2002
14. Vasioukhin V, Bauer C, Yin M, Fuchs E: Directed actin polymerization is the driving force for epithelial cell-cell adhesion. *Cell* 100: 209–219, 2000
15. Birkenfeld J, Kartmann B, Anliker B, Ono K, Schlotcke B, Betz H, Roth D: Characterization of zetin 1/rBSPRY, a novel binding partner of 14-3-3 proteins. *Biochem Biophys Res Commun* 302: 526–533, 2003
16. Muslin AJ, Tanner JW, Allen PM, Shaw AS: Interaction of 14-3-3 with signaling proteins is mediated by the recognition of phosphoserine. *Cell* 84: 889–897, 1996
17. Yaffe MB, Rittinger K, Volinia S, Caron PR, Aitken A, Leffers H, Gamblin SJ, Smerdon SJ, Cantley LC: The structural basis for 14-3-3:phosphopeptide binding specificity. *Cell* 91: 961–971, 1997
18. O'Kelly I, Butler MH, Zilberberg N, Goldstein SA: Forward transport. 14-3-3 binding overcomes retention in endoplasmic reticulum by dibasic signals. *Cell* 111: 577–588, 2002
19. Hoenderop JG, Muller D, Van Der Kemp AW, Hartog A, Suzuki M, Ishibashi K, Imai M, Sweep F, Willems PH, Van Os CH, Bindels RJ: Calcitriol controls the epithelial calcium channel in kidney. *J Am Soc Nephrol* 12: 1342–1349, 2001
20. Dardenne O, Prud'homme J, Arabian A, Glorieux FH, St-Arnaud R: Targeted inactivation of the 25-hydroxyvitamin D3–1alpha-hydroxylase gene (CYP27B1) creates an animal model of pseudovitamin D-deficiency rickets. *Endocrinology* 142: 3135–3141, 2001

Supplemental information for this article is available online at http://www.jasn.org/